

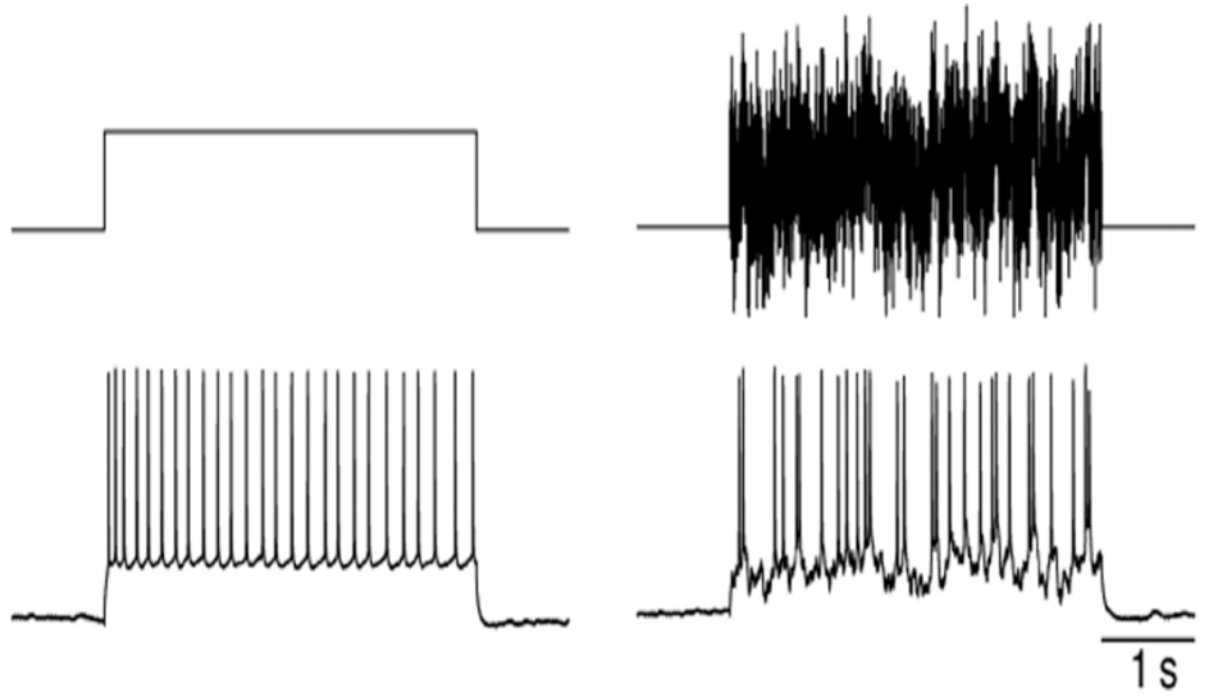
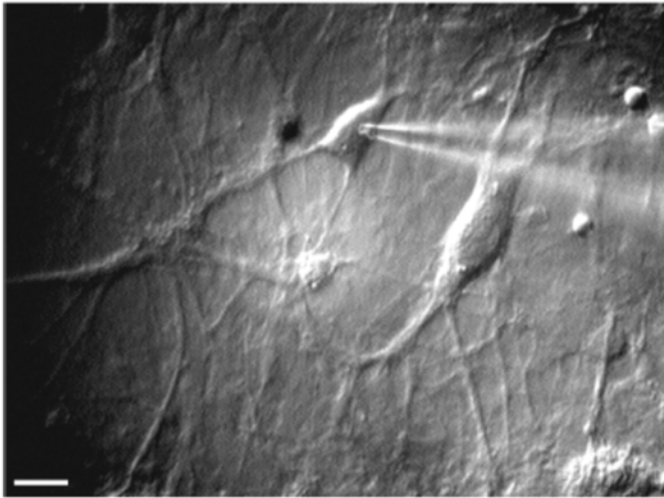
EXCITATORY AND INHIBITORY  
INTERACTIONS IN  
LOCALIZED POPULATIONS  
OF MODEL NEURONS

HUGH R. WILSON *and* JACK D. COWAN

*From the Department of Theoretical Biology, The University of Chicago,  
Chicago, Illinois 60637*

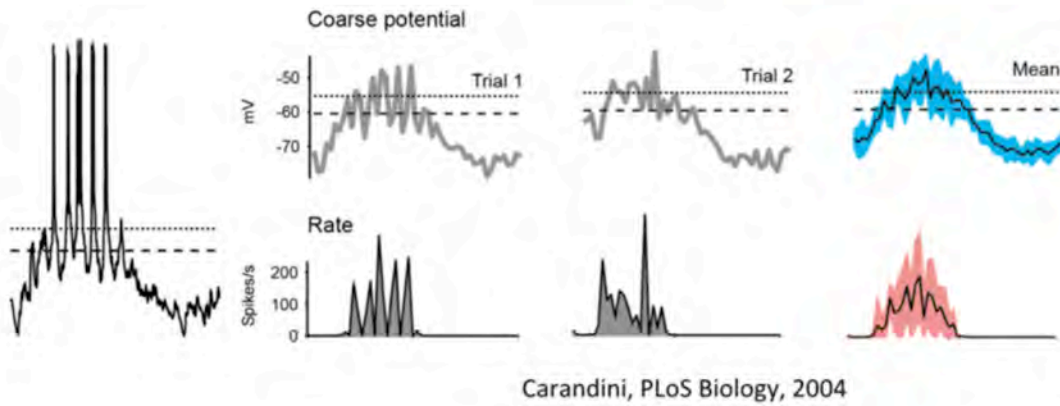
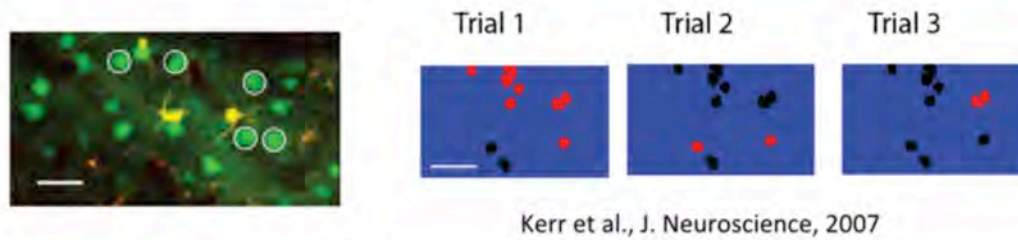
There is one final and crucial assumption upon which this study rests: *all nervous processes of any complexity are dependent upon the interaction of excitatory and inhibitory cells.* This assertion is supported by the work of Hartline and Ratliff (1958), Hubel and Wiesel (1963, 1965), Freeman (1967, 1968 *a, b*), Szentágothai (1967), and many others. In fact, this assumption is virtually a truism at this point, yet many neural modelers have dealt with nets composed entirely of excitatory cells (Beurle, 1956; Farley and Clark, 1961; ten Hoopen, 1965; Allanson, 1956). It was just this failure to consider inhibition that led Ashby et al. (1962) to conclude that the dynamical stability of the brain was paradoxical, and it was the introduction of inhibition by Griffith (1963) which dissolved the paradox. Consequently, we take it to be essential that there be both excitatory and inhibitory cells within any local neural population.

# Neuronal spiking - a threshold phenomena - is (largely) deterministic



Giugliano, Darbon, Arsiero, Luscher & Streit (J Neurophysiol 2004)

# Yet brain activity is noisy on every scale!



Liu et al., Neuron, 1999

## Cortical spiking in particular is irregular

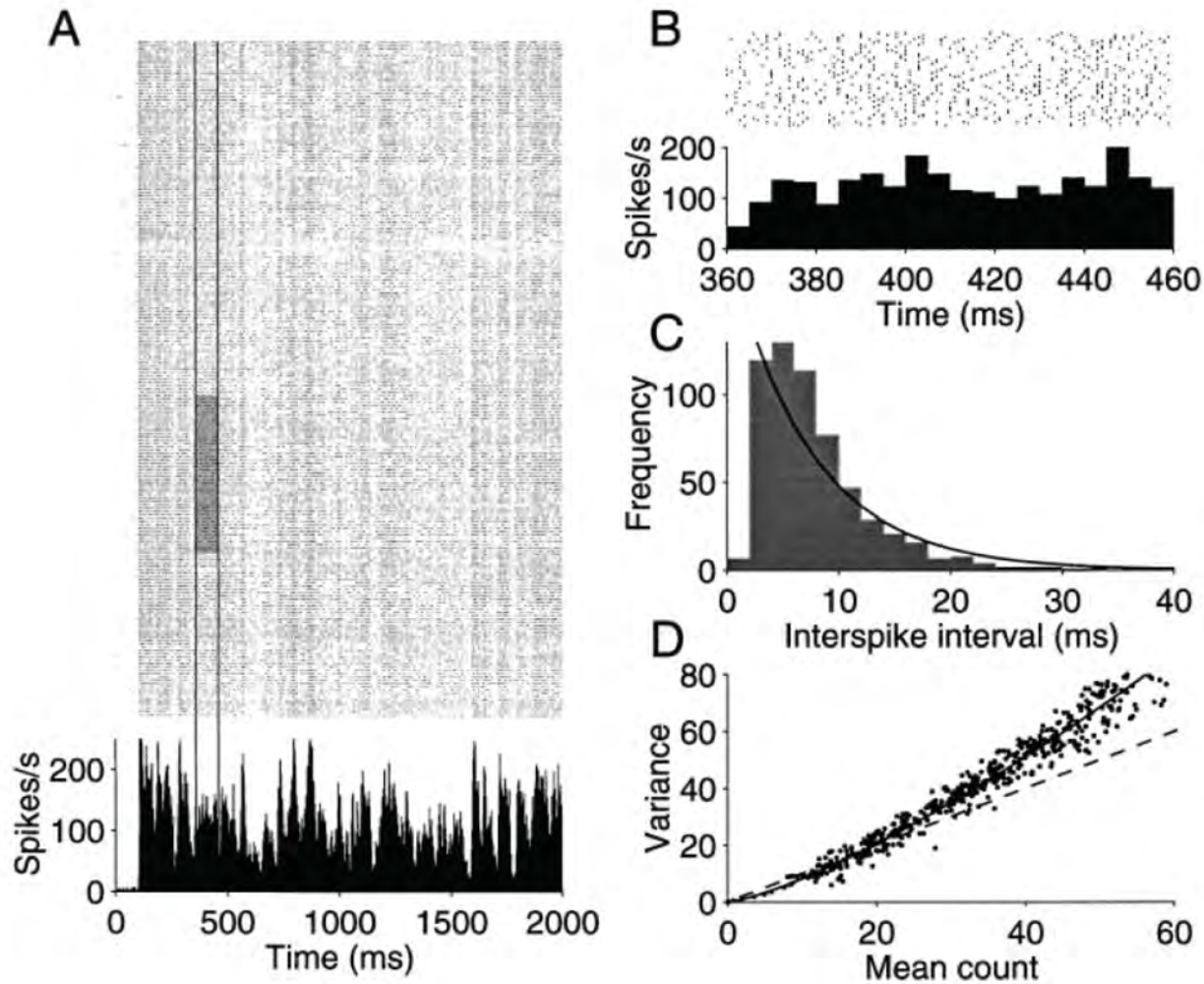
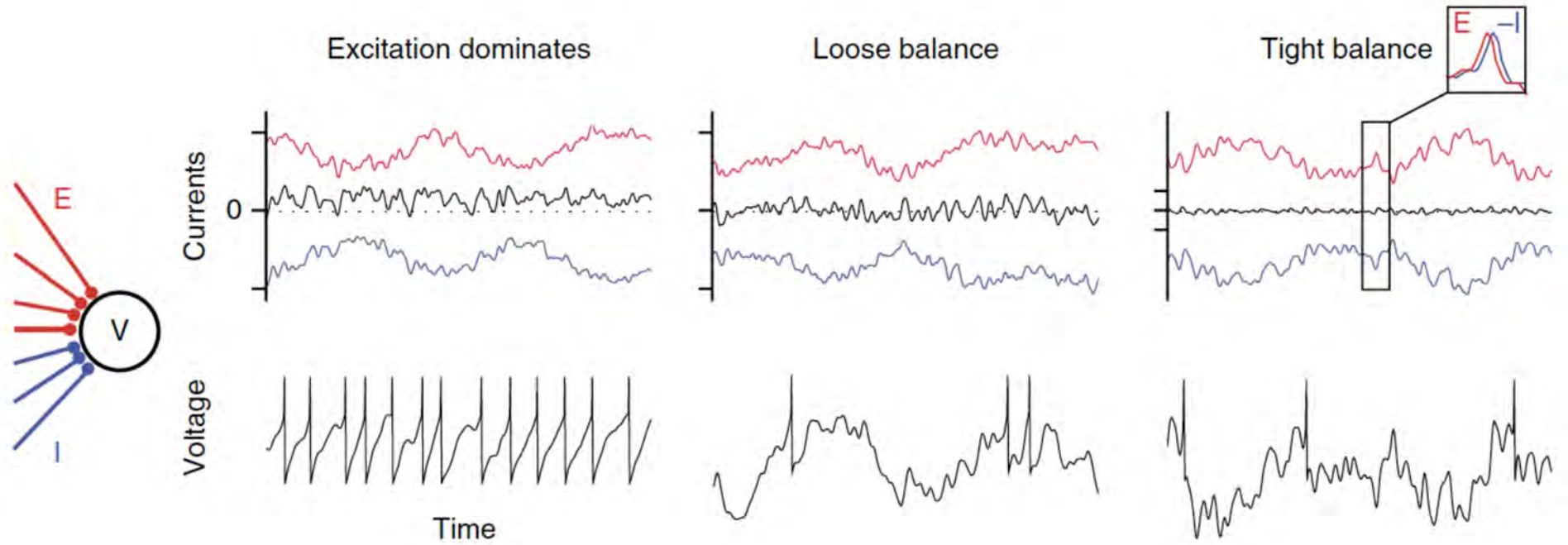


*Figure 1.* Response variability of a neuron recorded from area MT of an alert monkey. *A*, Raster and peristimulus time histogram (PSTH) depicting response for 210 presentations of an identical random dot motion stimulus. The motion stimulus was shown for 2 sec. Raster points represent the occurrence of action potentials. The PSTH plots the spike rate, averaged in 2 msec bins, as a function of time from the onset of the visual stimulus. The response modulates between 15 and 220 impulses/sec. *Vertical lines* delineate a period in which spike rate was fairly constant. The *gray region* shows 50 trials from this epoch, which were used to construct *B* and *C*. *B*, Magnified view of the shaded region of the raster in *A*. The spike rate, computed in 5 msec bins, is fairly constant. Notice that the magnified raster reveals substantial variability in the timing of individual spikes. *C*, Frequency histogram depicting the spike intervals in *B*. The *solid line* is the best fitting exponential probability density function. *D*, Variance of the spike count is plotted against the mean number of spikes obtained from randomly chosen rectangular regions of the raster in *A*. Each *point* represents the mean and variance of the spikes counted from 50 to 200 adjacent trials in an epoch from 100 to 500 msec long. The *shaded region* of *A* would be one such example. The best fitting power law is shown by the *solid curve*. The *dashed line* is the expected relationship for a Poisson point process.

Shadlen & Newsome (J Neurosci 1998)

# Balanced excitatory and inhibitory currents can lead to noisy input currents



Denuve & Machens (Nat Neuro 2016)



# Balanced currents are observed in vivo under numerous conditions

## Spatially Opponent Excitation and Inhibition in Simple Cells of the Cat Visual Cortex

David Ferster

Department of Neurobiology and Physiology, Northwestern University, Evanston, Illinois 60208

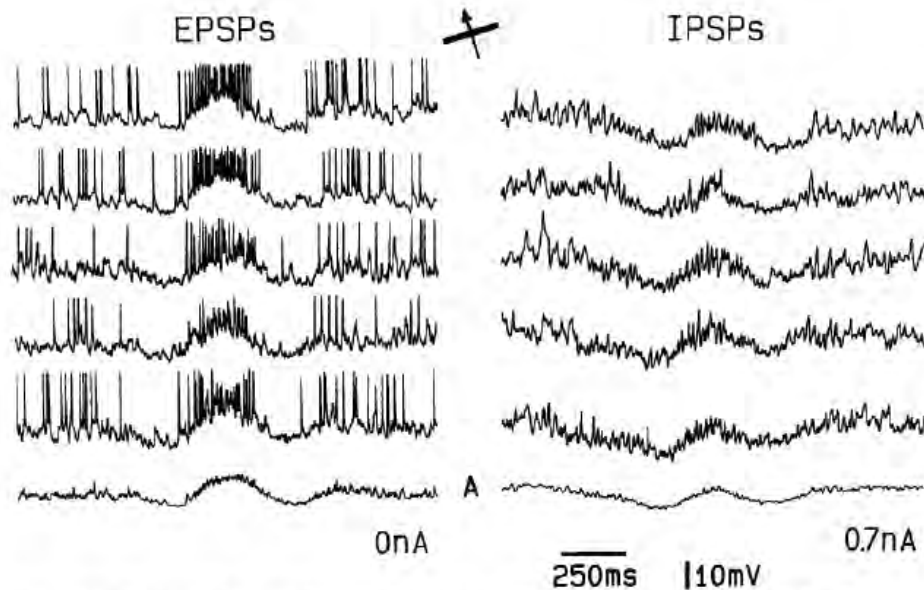


Figure 1. Intracellularly recorded responses of a simple cell evoked by a bright bar swept across its receptive field. The inset indicates the orientation and direction of motion of the stimulus. The bar measured  $0.75^\circ \times 6^\circ$  and traveled  $4^\circ$  in the 2 sec recorded in each trace. Whether EPSPs or IPSPs were visible in the records was controlled by the amount of current injected into the cell through the recording electrode. In this and all subsequent figures, the amount of current injected into the cell through the recording electrode while recording each set of traces is indicated to the lower right. EPSPs are shown to the left (0 nA), IPSPs to the right (0.7 nA). The bottom trace in each column (A) represents an average of 10 individual records.

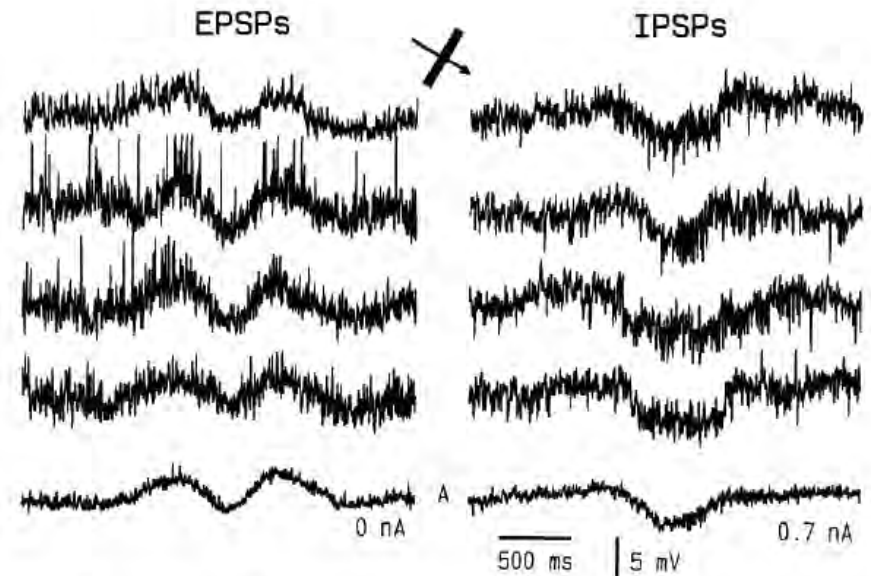


Figure 3. Responses to a moving bright bar recorded intracellularly from a second simple cell. The receptive field of this cell consisted of 2 ON regions flanking a central OFF region. The bar moved at a rate of  $2^\circ/\text{sec}$ .

Ferster (J Neurosci 1988)

# Balanced currents are observed in vivo under numerous conditions

## Instantaneous Modulation of Gamma Oscillation Frequency by Balancing Excitation with Inhibition

Bassam V. Atallah<sup>1,\*</sup> and Massimo Scanziani<sup>2,\*</sup>

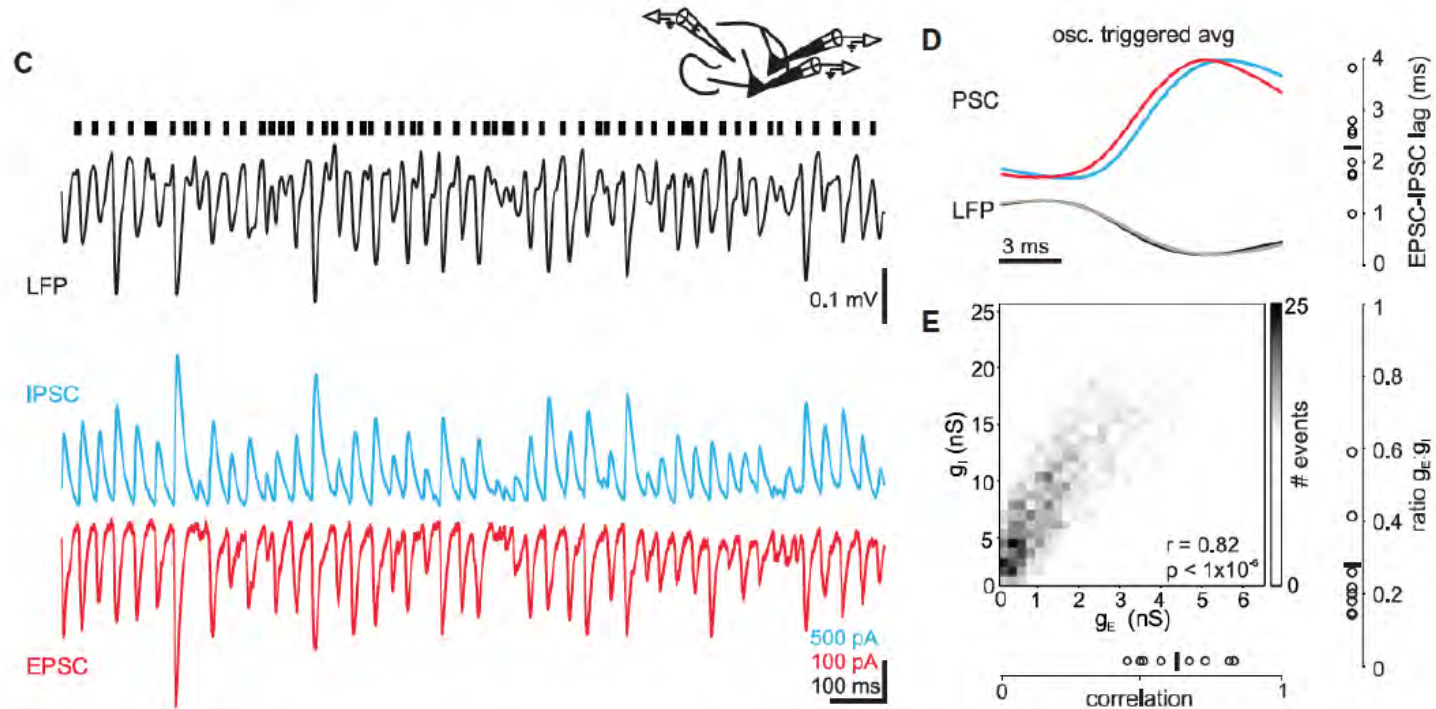


**Figure 2. Excitation Instantaneously Balanced by Proportional Inhibition during Each Gamma Oscillation Cycle**

(C) Dual patch-clamp recording from two neighboring CA3 pyramidal cells. Oscillations are monitored with an LFP electrode (black, positivity is up). EPSCs (red) and IPSCs (cyan) simultaneously recorded by holding two cells at the reversal potential for inhibition ( $-3$  mV) and excitation ( $-87$  mV), respectively. Note the correlated fluctuations in the amplitude of excitation and inhibition.

(D) (Left) Average time course of EPSC and IPSC (same cell as C) during an oscillation cycle recorded in the LFP, i.e., oscillation triggered average. EPSC is inverted for illustration purposes. LFPs recorded simultaneously with EPSCs and IPSCs are shown as black and gray traces, respectively. (Right) Summary of EPSC-IPSC lag during an oscillation cycle. Horizontal bar is the average.

(E) (Top) Cycle-by-cycle correlation between excitatory and inhibitory conductances recorded in the pair shown in (C). Summary of correlation between excitation and inhibition (bottom) and ratio of mean excitatory and inhibitory conductances (right) ( $n = 8$  pairs). Vertical and horizontal bars illustrate respective averages.

# Neocortical Network Activity *In Vivo* Is Generated through a Dynamic Balance of Excitation and Inhibition

Bilal Haider, Alvaro Duque, Andrea R. Hasenstaub, and David A. McCormick

Department of Neurobiology, Kavli Institute for Neuroscience, Yale University School of Medicine, New Haven, Connecticut 06510

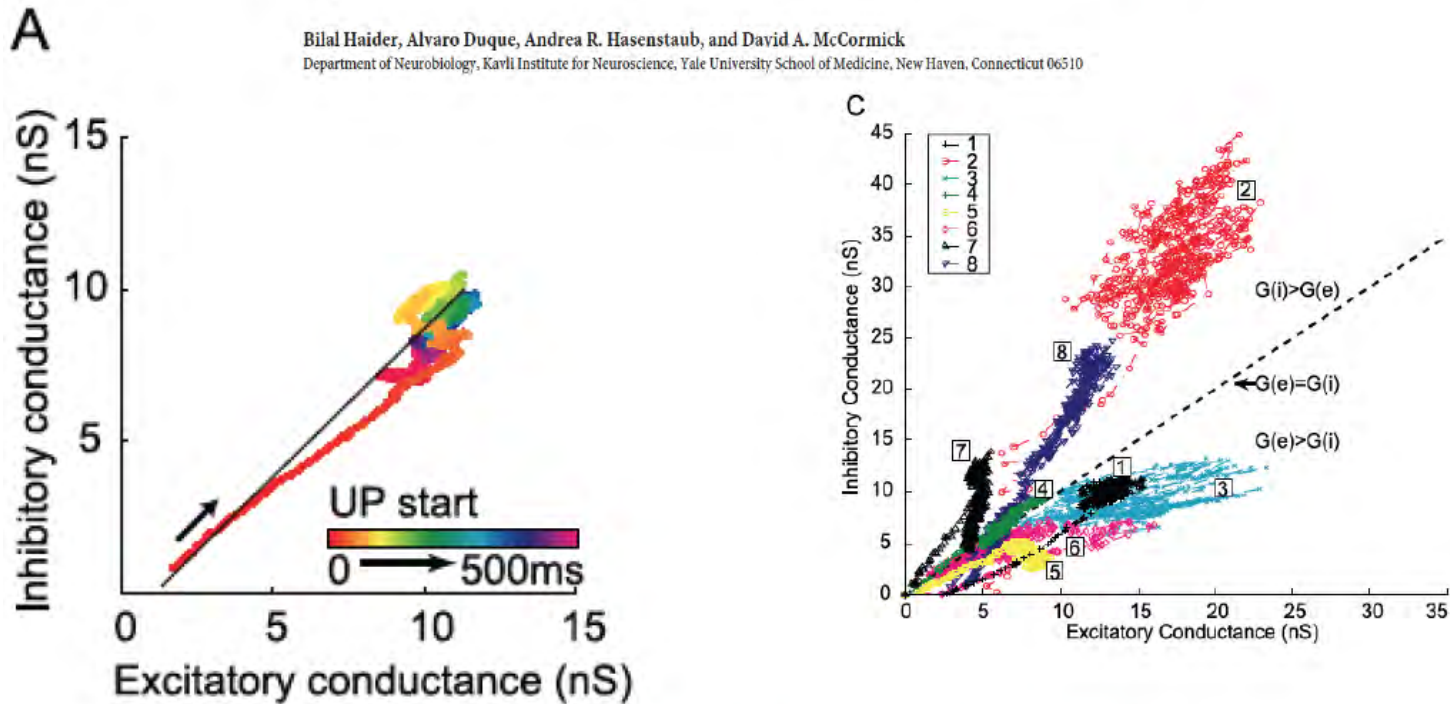
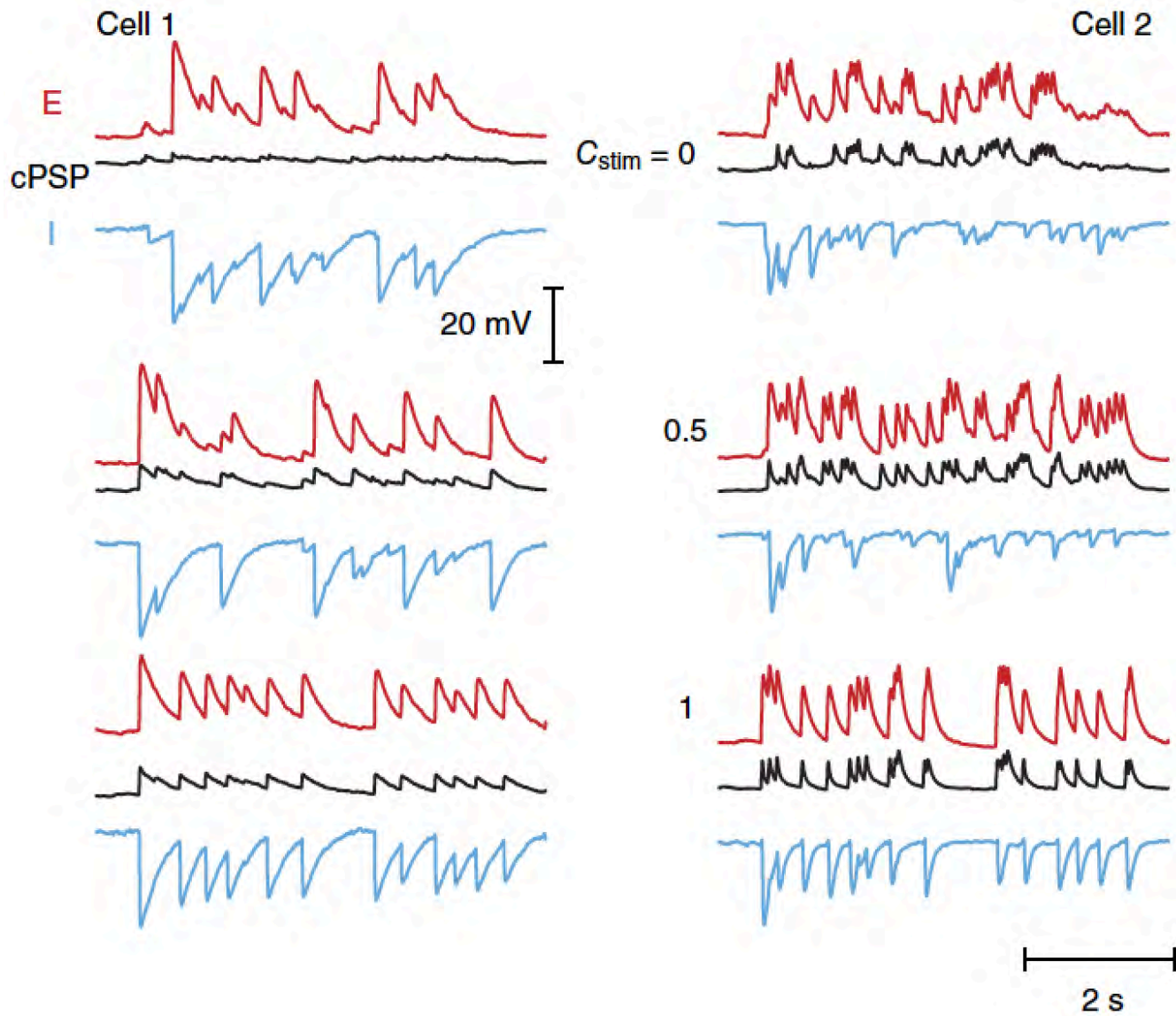


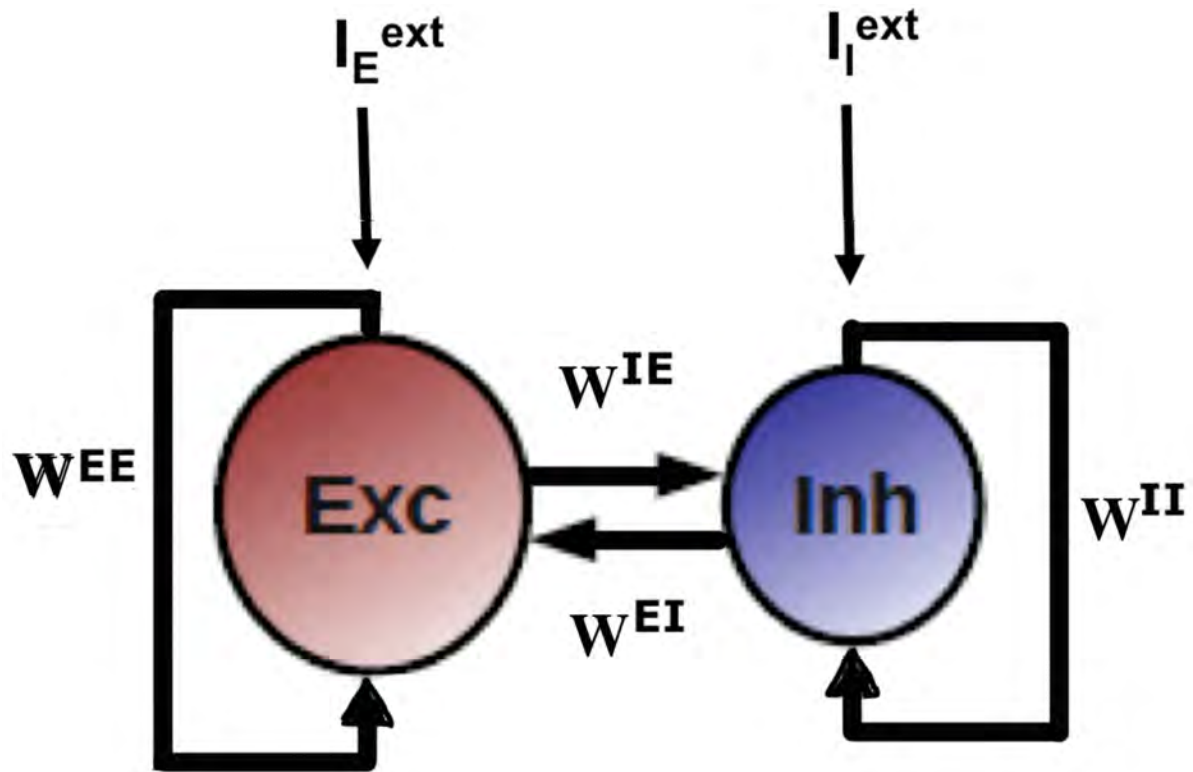
**Figure 7.** Excitatory and inhibitory conductances are proportional and balanced during Up states. **A**, Plot of calculated excitatory and inhibitory conductances in a single neuron during the course of the Up state (0–500 ms, indicated by progressive movement through color bar) shows that excitation and inhibition remain proportional and nearly equal despite large changes in total conductance (slope of linear fit,  $m = 0.98$ ;  $r^2 = 0.78$ ). Note that the start of the Up state shows a deviation toward excitation, but rapidly swings toward inhibition and thereafter exhibits a balance between the two.

**C**, Excitation and inhibition are proportional and balanced both within and across neurons during recurrent network activity. Scatterplot of excitatory versus inhibitory conductances for a population of neurons ( $n = 8$ ), calculated for 500 ms from the start of the Up state. Note the linear relationship for each individual neuron, as well as the clustering around a ratio of equal excitatory and inhibitory conductances ( $G_e = G_i$ ; dashed line; 4 of 8 cells biased toward excitation, 3 of 8 cells toward inhibition, 1 of 8 cells approximately equal; population reversal potential,  $-37.2 \pm 6.5$  mV).



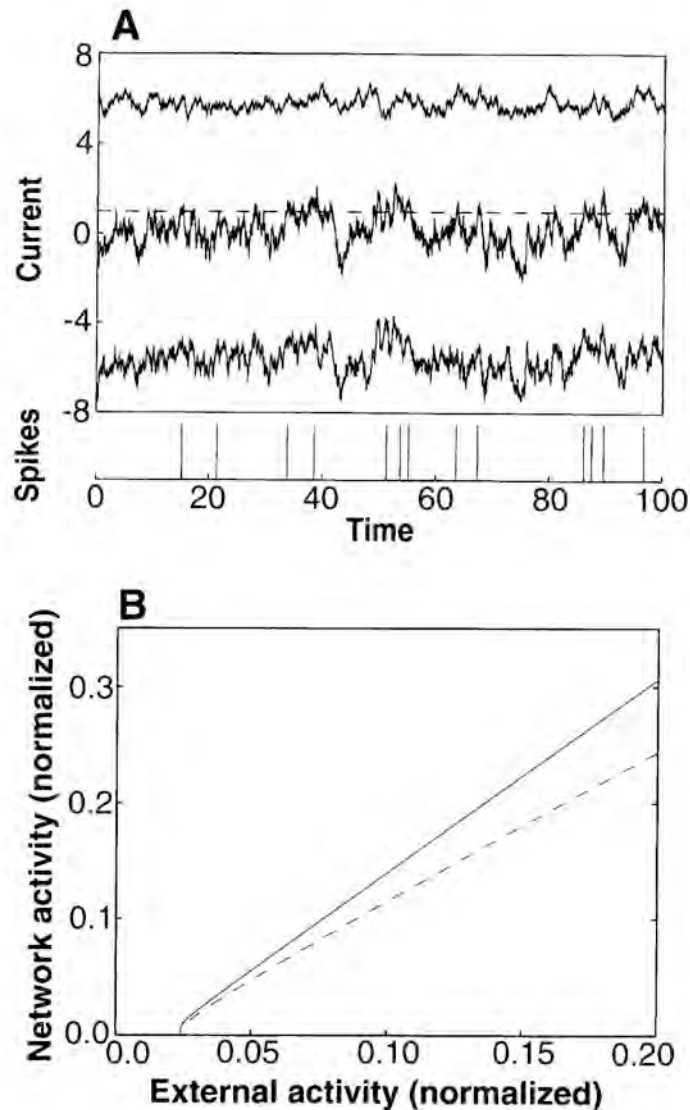


### Network model



van Vresswijk & Sompolinsky (Science 1996; J Comp Neurosci 1998)

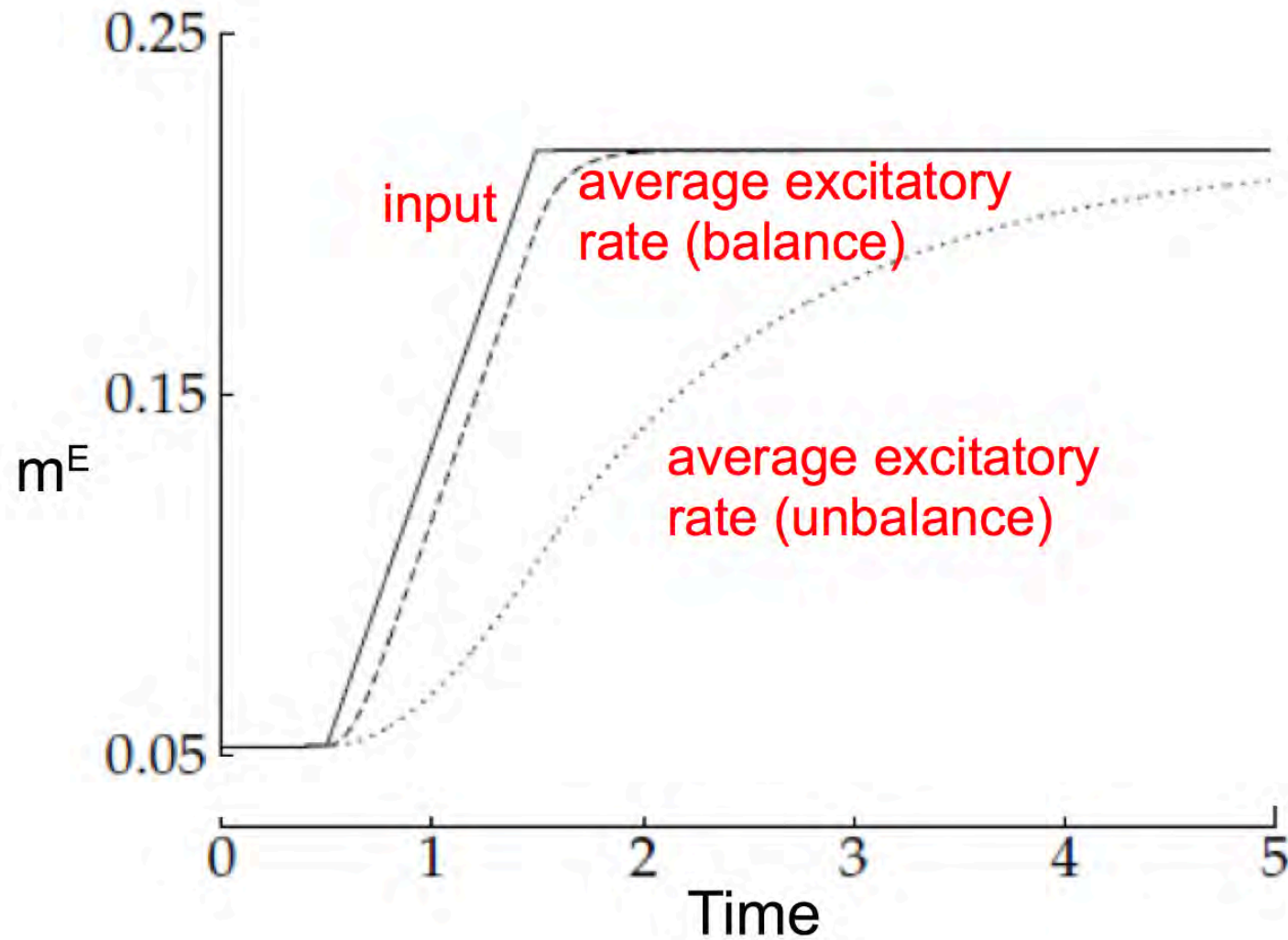
## Results for Output-Input network activity



(A) Temporal structure of the inputs and activity of a single excitatory unit. The upper panel shows the total excitatory input (consisting of external input and excitatory feedback) (upper trace) and the total inhibitory input (lower trace), as well as the net input (middle trace). The currents are shown in units of the threshold (dashed line). They were calculated by sampling from the Gaussian statistics of the currents predicted by the theory.

Below, the times when the cell switched to the active state are indicated. The cell is set to the active state when a suprathreshold net input coincides with the update time of the cell. (B) The mean activity of the excitatory neurons (solid line) and the inhibitory ones (dashed line) as functions of the activity of the external units. The activities shown here and in the following figures correspond to firing rates divided by their maximum value. Assuming a neuronal maximum rate of 1000 Hz, a mean activity of 0.1 corresponds to a firing rate of 100 Hz.

The increase in noise is accompanied by an increase in response speed of  $m^E$  and  $m^I$  to an input

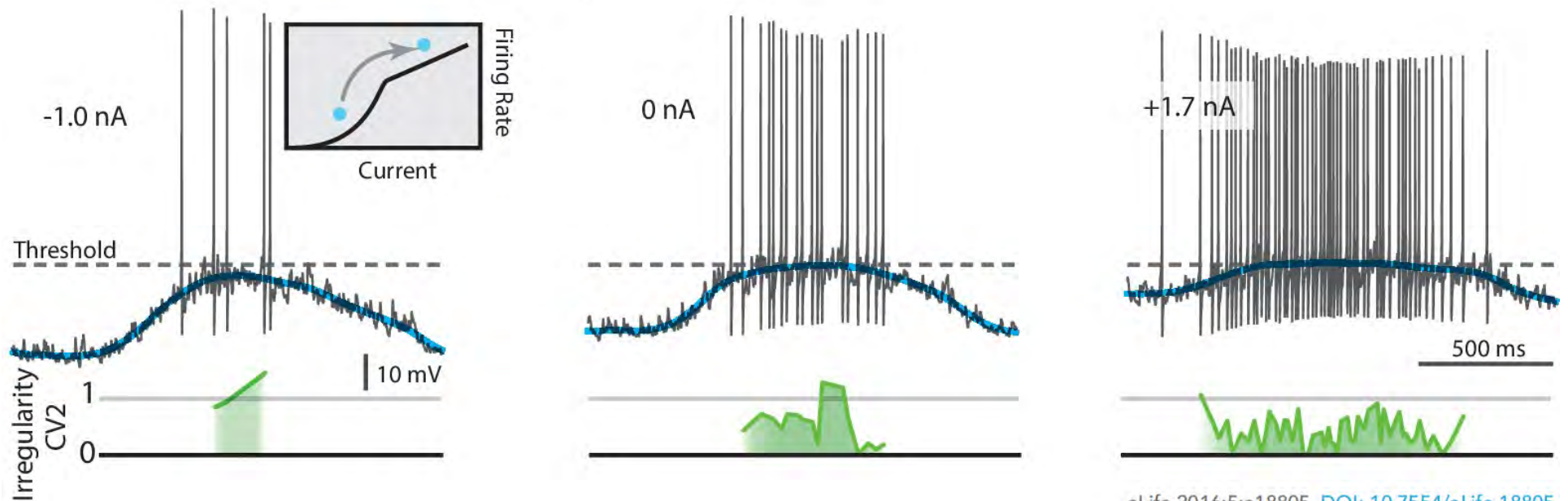




Neuronal spiking is best driven by noise with the mean input near threshold

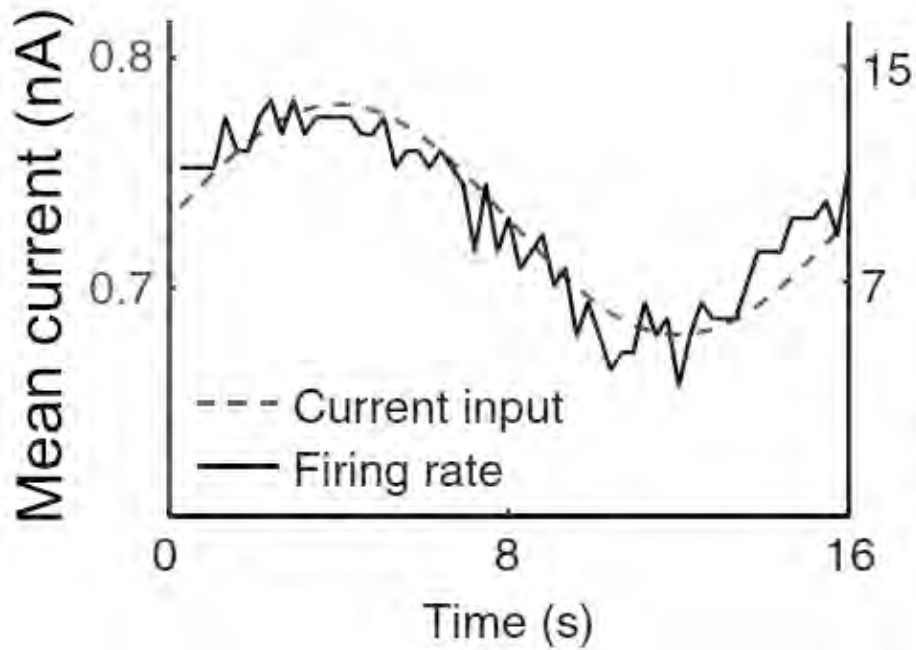
## Lognormal firing rate distribution reveals prominent fluctuation-driven regime in spinal motor networks

Peter C Petersen, Rune W Berg

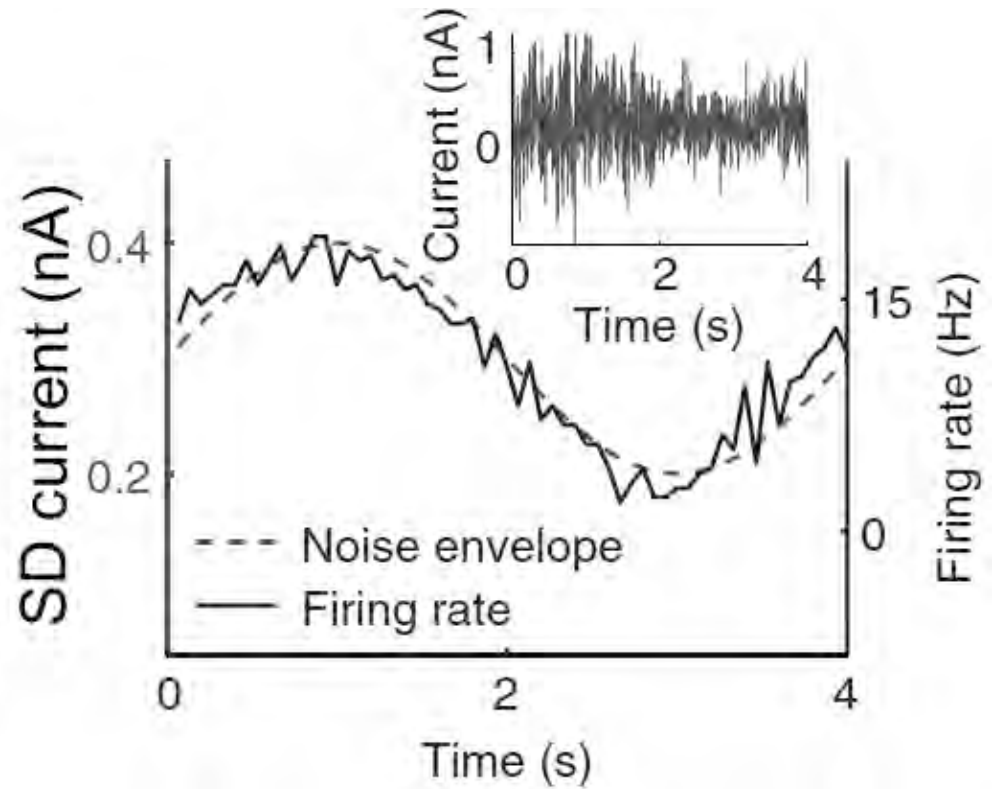


# Neuronal spiking driven by the envelope of noise

## Super-threshold changes in mean

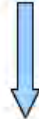


## Sub-(but near)-threshold mean plus noise



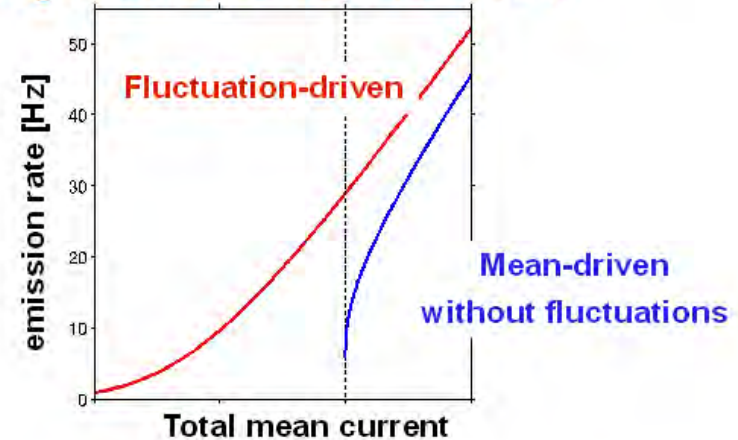
# Firing Rates of Single Neurons in the *Balanced* Regime

Average current is sub-threshold and spikes are triggered by fluctuations

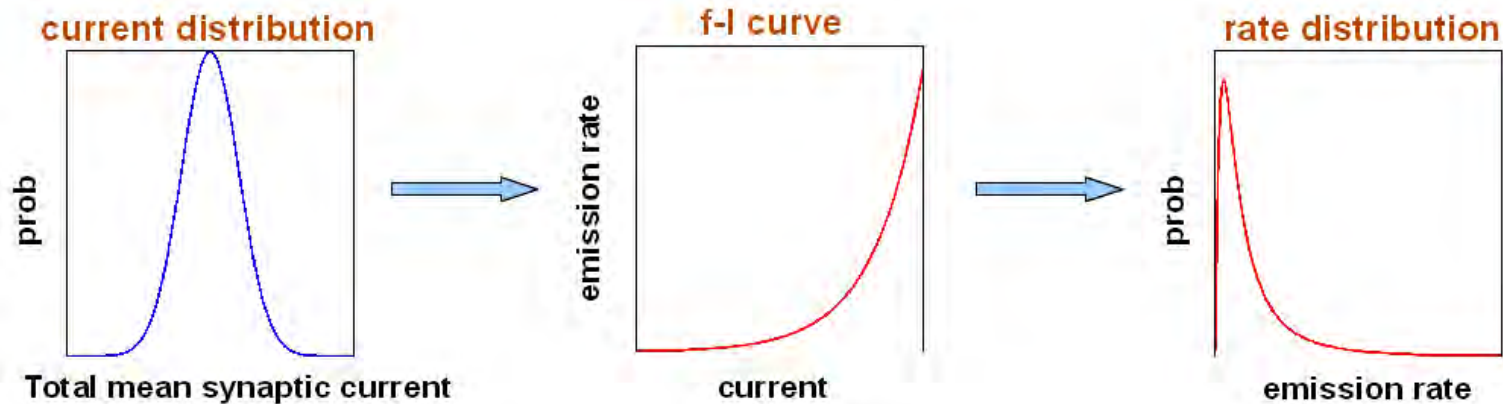


spiking is temporally irregular

Single neuron effective f-I curve

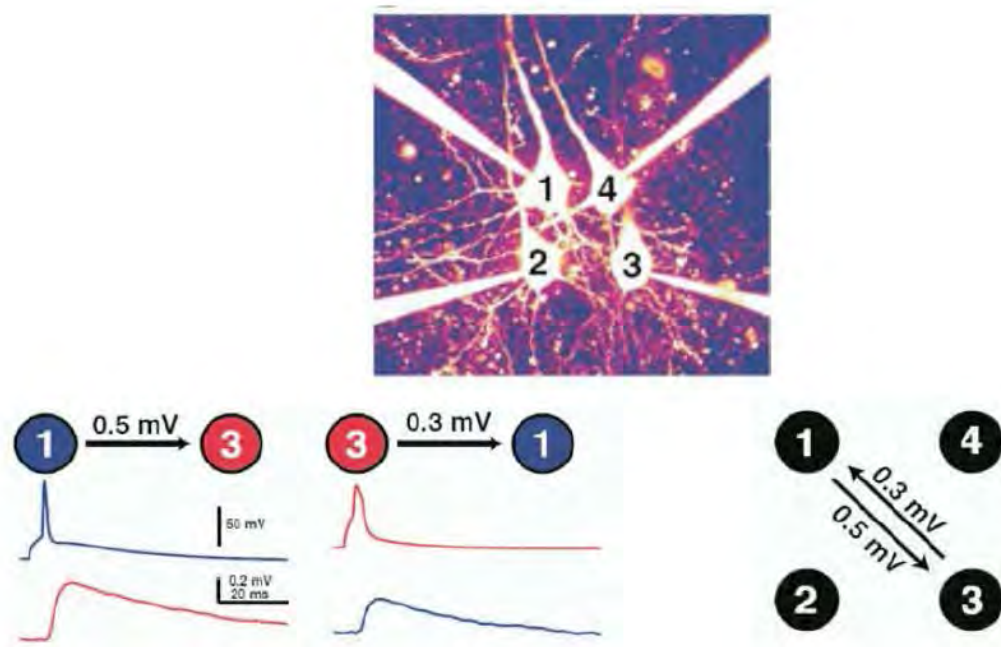


concavity of the f-I curve makes the rates' distribution right-skewed



# Why is this all not so simple to understand?

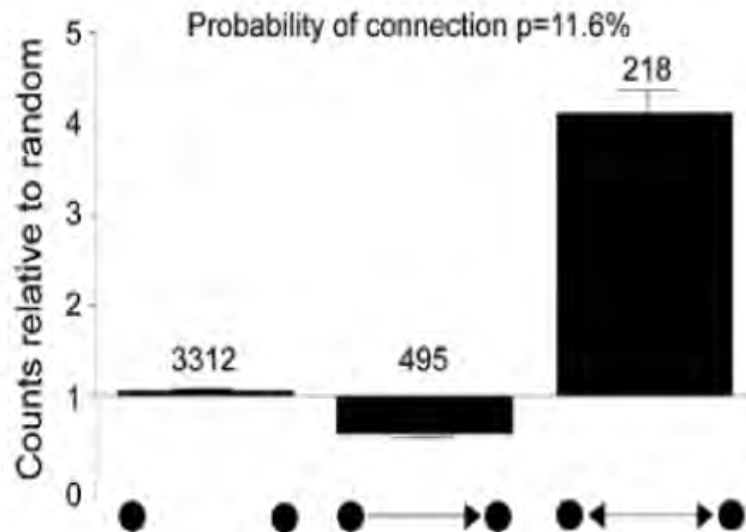
- Connections are dense, non-randomly distributed and nonrandomly weighted
- Few strong connections in a sea of weak connections



- Information about the presence and strength of connections
- But false negatives due to slicing artefacts

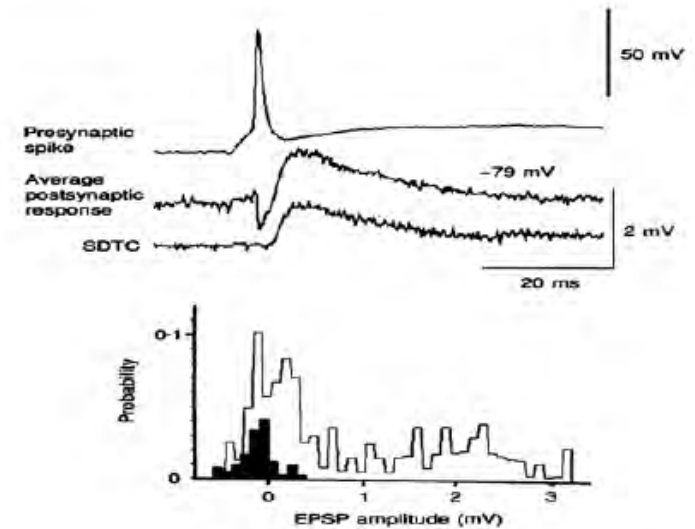


## Overrepresentation of bidirectional motifs



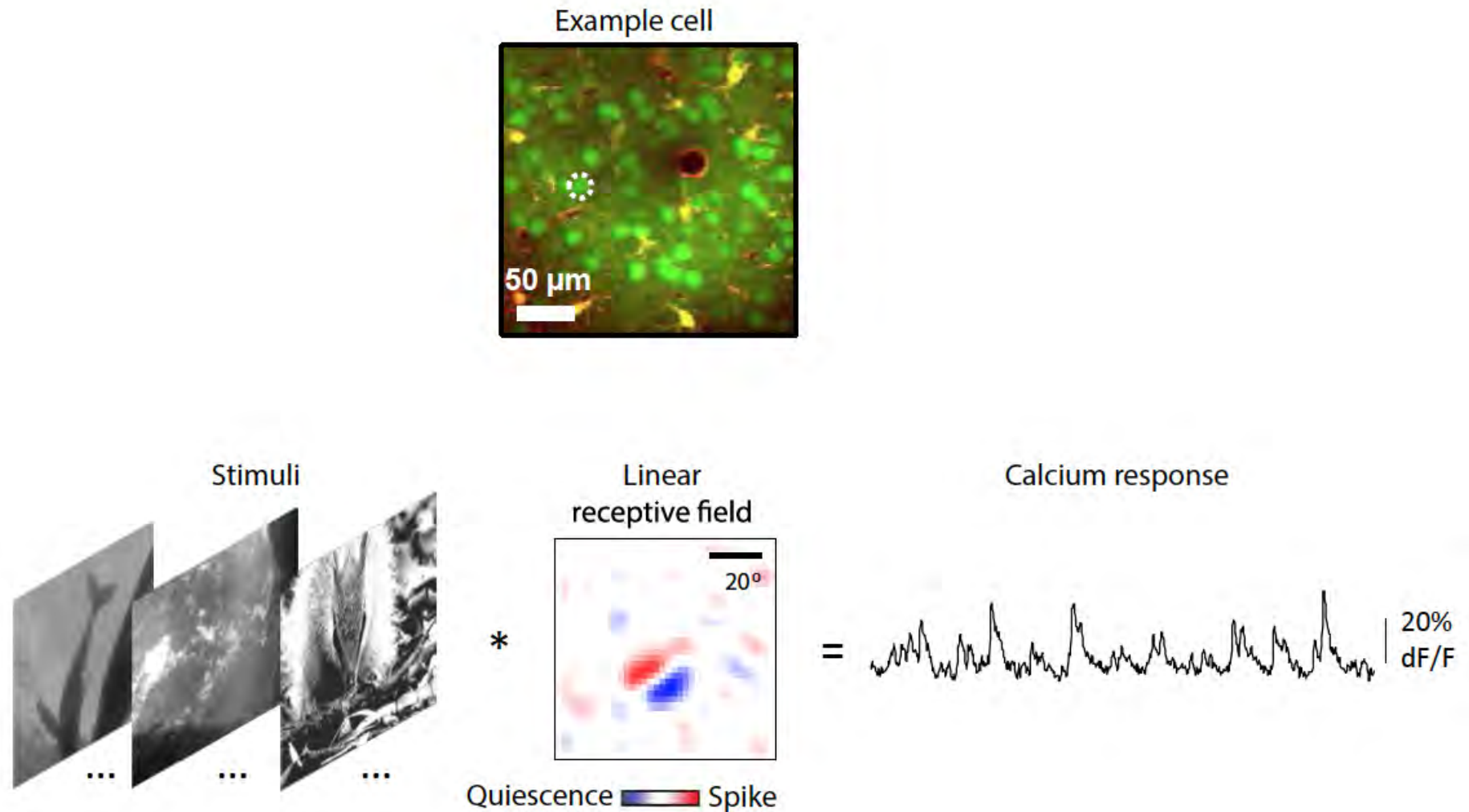
L5 pyramidal cells, Song et al. (2005)

## Connection strengths are variable and their distribution has a long tail

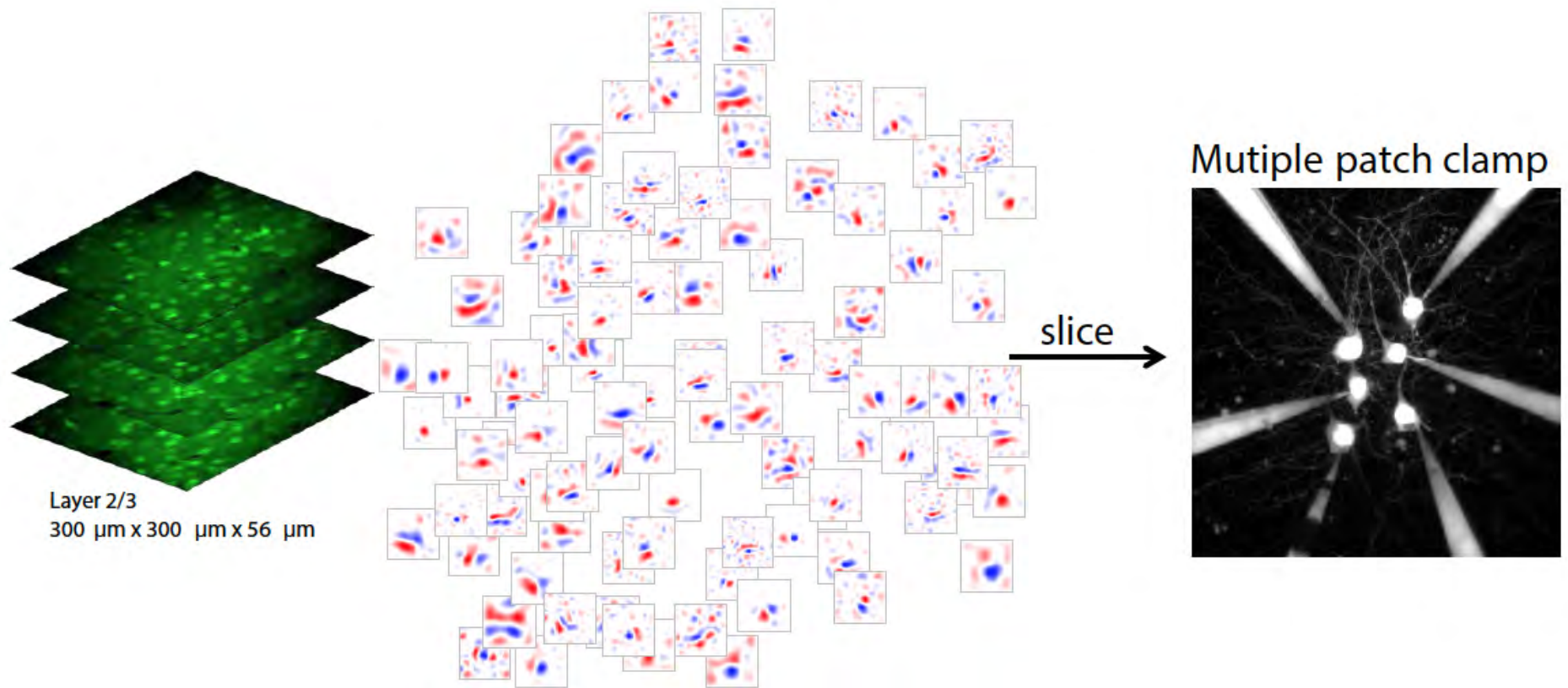


L5/6 pyramidal cells, Deuchars, West, Thomson (1994)

# Mapping receptive fields with two-photon calcium imaging and reverse correlation

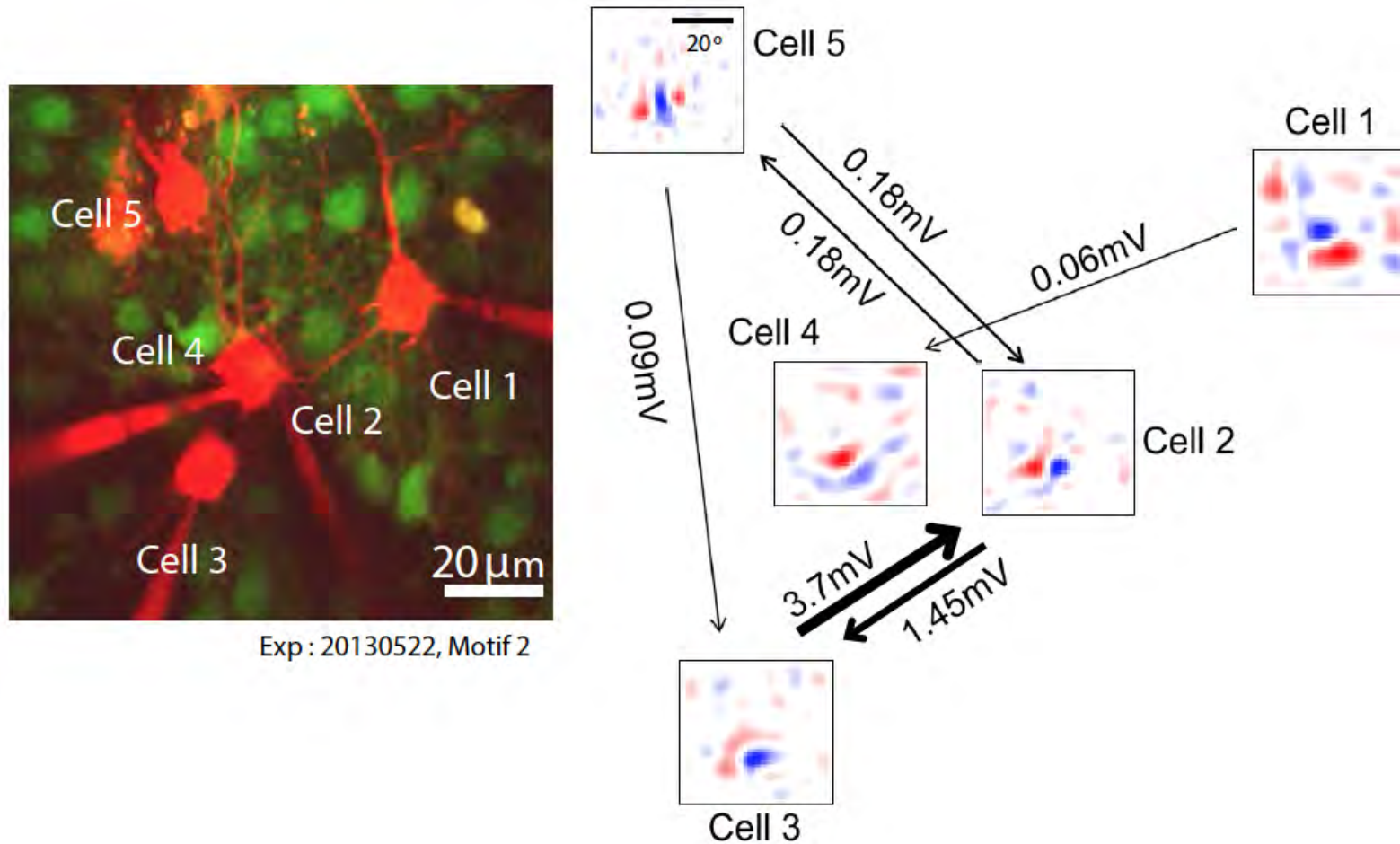


Cossell, Iacaruso, Muir, Houlton, Sader, Ko, Hofer & Mrsic-Flogel (Nature 2015)



Cossell, Iacaruso, Muir, Houlton, Sader, Ko, Hofer & Mrsic-Flogel (Nature 2015)

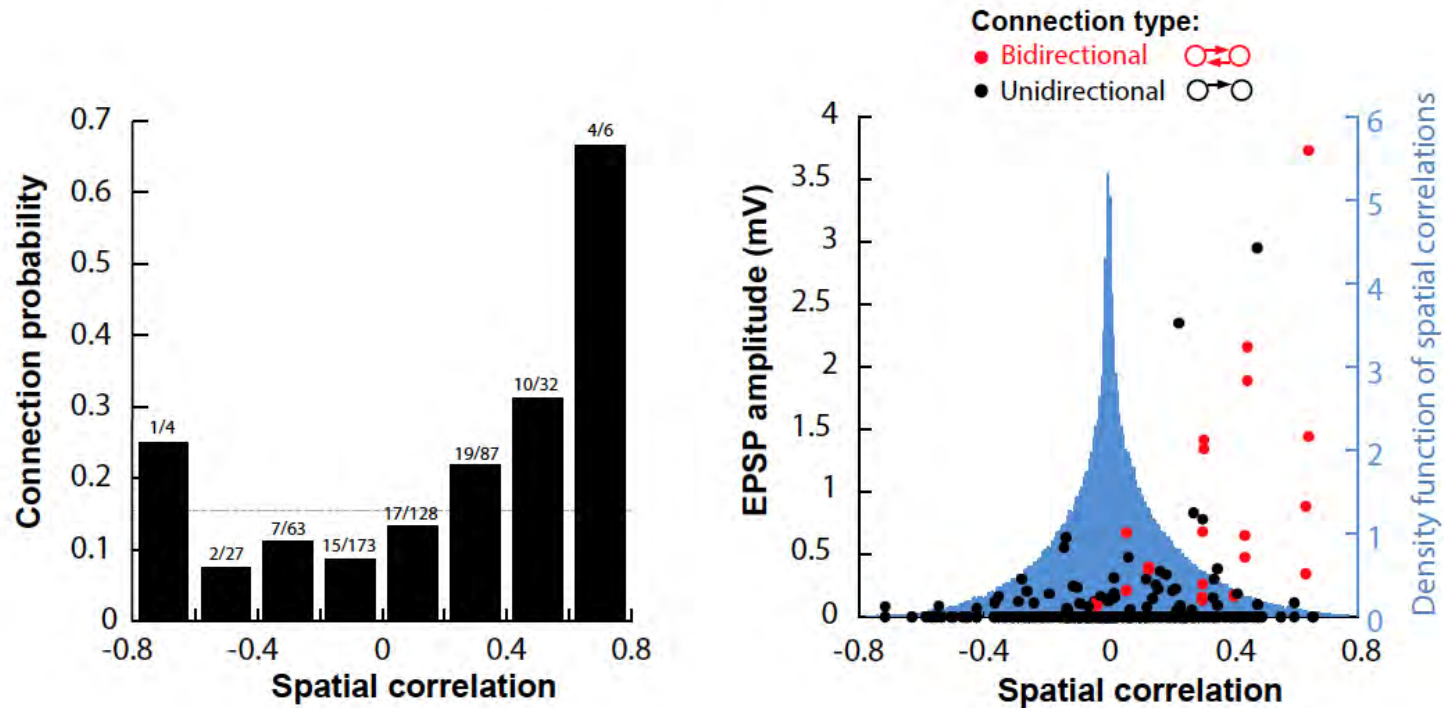
# Relating synaptic connections to receptive fields



Cossell, Iacaruso, Muir, Houlton, Sader, Ko, Hofer & Mrsic-Flogel (Nature 2015)



## Similarity of receptive fields predicts probability, strength, and reciprocity of synaptic connections



Spatial correlation is a strong predictor of connectivity

Cell pairs with positive correlations are more likely to connect with strong connections

Reciprocal connections are stronger and exist between cell pairs with similar receptive fields

Cossell, Iacaruso, Muir, Houlton, Sader, Ko, Hofer & Mrsic-Flogel (Nature 2015)